

# Reaction of CH with H<sub>2</sub>O: Temperature Dependence and Isotope Effect

Mark A. Blitz, Michèle Pesa, Michael J. Pilling,\* and Paul W. Seakins

School of Chemistry, University of Leeds, Leeds LS2 9JT, U.K.

Received: February 1, 1999; In Final Form: April 23, 1999

The reactions of CH( $\nu=0$ ) and CD( $\nu=0$ ) radicals with H<sub>2</sub>O and D<sub>2</sub>O were investigated in the temperature range between 291 and 723 K. The reactions of CH( $\nu=1$ ) and CD( $\nu=1,2$ ) with H<sub>2</sub>O and D<sub>2</sub>O were studied at 293 K. CH(D) radicals were generated by multiphoton dissociation of CH(D)Br<sub>3</sub> using pulsed laser photolysis and the resulting CH(D) time profiles were monitored by laser induced fluorescence. The reactions of CH(D) in the  $\nu = 0$  state exhibit a negative temperature dependence and are independent of total pressure between 20 and 200 Torr at room temperature. The rate coefficients can be fitted over the experimental temperature range by the following expressions:  $k(T)_{\text{CH}+\text{H}_2\text{O}} = (1.56 \pm 0.25) \times 10^{-11}(T/298)^{-1.42 \pm 0.31} \text{ cm}^3 \text{ molecule}^{-1} \text{ s}^{-1}$ ;  $k(T)_{\text{CH}+\text{D}_2\text{O}} = (1.49 \pm 0.25) \times 10^{-11}(T/298)^{-1.04 \pm 0.29} \text{ cm}^3 \text{ molecule}^{-1} \text{ s}^{-1}$ ;  $k(T)_{\text{CD}+\text{H}_2\text{O}} = (1.38 \pm 0.21) \times 10^{-11}(T/298)^{-1.16 \pm 0.25} \text{ cm}^3 \text{ molecule}^{-1} \text{ s}^{-1}$ ;  $k(T)_{\text{CD}+\text{D}_2\text{O}} = (1.71 \pm 0.28) \times 10^{-11}(T/298)^{-1.13 \pm 0.32} \text{ cm}^3 \text{ molecule}^{-1} \text{ s}^{-1}$ . The errors on the parameters correspond to  $\pm 1 \sigma$  standard deviation from nonlinear least-squares fitting, and the data were weighted by  $1/\sigma^2$  using a  $\sigma$  of 20%. Deuteration of either the CH radical or H<sub>2</sub>O has no discernible effect on the kinetics of the reaction, suggesting formation of an intermediate complex prior to the insertion of CH(D) into the OH(D) bond. Rate coefficients for CH( $\nu=1$ ) and CD( $\nu=1,2$ ) were found to be faster than those for the radicals in the vibrational ground state. The results are compared with previous experimental and theoretical studies, and the mechanism is discussed.

## I. Introduction

The CH radical is an important species in hydrocarbon combustion systems<sup>1–3</sup> and planetary atmospheres.<sup>4–6</sup> For example, its high heat of formation ( $\Delta_f H^\circ_{298} = 596.4 \text{ kJ mol}^{-1}$ ) results in an exothermic reaction with molecular nitrogen, which is the initial step in the formation of prompt NO in flames. For accurate modeling of combustion systems, comprehensive knowledge of the kinetics and mechanisms of CH reactions as a function of temperature and pressure is required. Therefore, extensive experimental and theoretical studies have been undertaken to investigate the kinetics and mechanisms of CH reactions with many important species.<sup>7–13</sup> Recently, we investigated the kinetics of the CH + CH<sub>4</sub><sup>14</sup> reaction, which was suggested to proceed through CH insertion into a C–H bond of CH<sub>4</sub>.<sup>15–18</sup> Many other CH reactions were rationalized via initial insertion into the reactant before rearrangement of the activated intermediate.<sup>19</sup>

In the present work we investigate the reaction of CH radicals with H<sub>2</sub>O, another important species in hydrocarbon combustion. To date, there has been one study of the temperature dependence of this reaction<sup>20</sup> and also a room-temperature measurement.<sup>21</sup> This reaction is believed to occur initially via CH insertion into the O–H bond of H<sub>2</sub>O; the abstraction channel is endothermic (see Table 4) and will be slow. An insertion mechanism was also suggested by a theoretical study,<sup>22</sup> which also pointed out an interesting feature in the reaction path: an intermediate complex prior to the transition state was found that is lower in energy than the reactants. It was suggested that this complex involves a donation of the lone pair on the O-atom to the empty carbon *p*-orbital of the CH radical.

We have studied the reactions of CH( $\nu=0$ ) and CD( $\nu=0$ ) radicals with H<sub>2</sub>O and D<sub>2</sub>O in the temperature range between

291 and 723 K and also of CH( $\nu=1$ ) and CD( $\nu=1,2$ ) with H<sub>2</sub>O and D<sub>2</sub>O at 293 K. The results on the different isotopic variations provide insight into the possible mechanism of the CH reaction with H<sub>2</sub>O.

## II. Experimental Section

A conventional laser flash photolysis/laser-induced fluorescence (LIF) technique in a quasistatic cell was used to measure the CH kinetics. This experimental setup was similar to that used in our previous studies on the CH radical.<sup>14,23</sup>

Briefly, the CH(D) radicals were generated by multiphoton photolysis of bromoform, CH(D)Br<sub>3</sub>, using the unfocused 248 nm output of a KrF excimer laser (Lambda Physik, LPX 100) operating at 5 Hz. The laser energies were typically ca. 150 mJ/pulse. The relative concentrations of CH(D)( $\nu=0,1,2$ ) radicals were monitored by LIF, using either the  $B^2\Sigma^- \leftarrow X^2\Pi$  electronic transition at ca. 390 nm or the  $A^2\Delta \leftarrow X^2\Pi$  transition at ca. 430 nm. The appropriate transitions for probing the CH-(D)( $\nu=1,2$ ) concentrations were selected by using the known literature spectroscopy on the *A* state.<sup>24–26</sup> For CH( $\nu=0$ ) both *A* and *B* state transitions were used and gave identical results. The probe laser was a Nd:YAG (Spectron SL 803, doubled output at 532 nm) pumped dye laser (Spectron 4000 G) operating on either DCM (ca. 615 nm) or Pyridine I (ca. 720 nm). The probe light was generated by frequency mixing the red output from the dye laser with the infrared output (1064 nm) from the Nd:YAG laser, using a KDP crystal. The fluorescence was filtered by a monochromator ( $\pm 10 \text{ nm}$ ) and detected at right angles to the lasers by a photomultiplier (EMI 9813 QKB). The signal from the photomultiplier was integrated by a boxcar averager (SRS SR250), digitized and stored on a personal computer.

The CH(D) time profiles were obtained by varying the delay time between the photolysis and probe lasers using a home-

\* E-mail: m.j.pilling@chem.leeds.ac.uk.

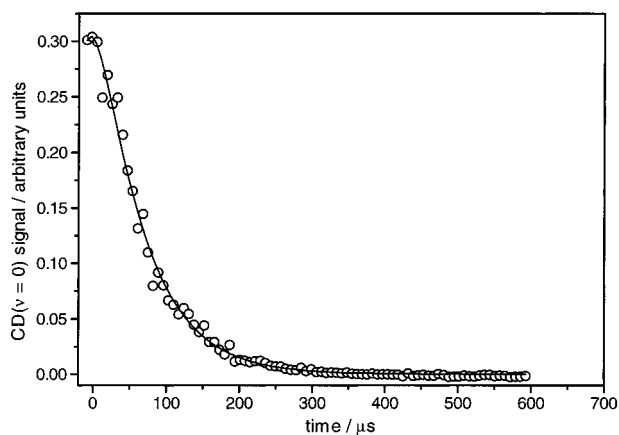


**Figure 1.** Typical time profile for  $\text{CD}(v=0)$ . The line represents a fit to the double exponential equation (1).

built delay generator, which was controlled by a PC. The decay traces contained typically 100 points that were recorded in 1.0–15  $\mu\text{s}$  increments and averaged over 7–12 shots per point.

The reaction cell was a metal six-way cross, which was heated by cartridge heaters in the temperature range between 291 and 723 K. The temperature was monitored by type K thermocouples positioned slightly above and below the laser beams and was known to better than  $\pm 5$  K.

Gas flows were measured by calibrated mass flow controllers. They were premixed with helium in a manifold before entering the reaction cell. Pressure in the cell was adjusted by a needle valve and measured using capacitance manometers (MKS). Experiments were performed in the pressure range 20–200 Torr.  $\text{CHBr}_3$  (Aldrich) and  $\text{CDBr}_3$  (99% D, Aldrich) were degassed and diluted with helium (CP grade, 99.999%, BOC) to 0.2% mixtures and stored in darkened 5 L glass bulbs.  $\text{CH(D)Br}_3$  partial pressures were typically ca. 0.2 mTorr.  $\text{H}_2\text{O}$  was distilled and deionized.  $\text{D}_2\text{O}$  (99% D, Aldrich) was used without further purification.

$\text{H}_2\text{O}$  and  $\text{D}_2\text{O}$  were transferred into the gas phase by flowing helium through a thermostated Dreschel bottle, containing either  $\text{H}_2\text{O}$  or  $\text{D}_2\text{O}$ , located before the mass flow controller (MFC). The gas flow before the MFC was demonstrated to be saturated by a humidity probe (Vaisala, HMP 230). The  $\text{H}_2\text{O}/\text{D}_2\text{O}$  concentrations were calculated by measuring the pressure before the MFC and the temperature of the thermostated Dreschel bottle, giving the  $\text{H}_2\text{O}$  concentration via its known vapor pressure.<sup>27,28</sup> The temperature of the Dreschel bottle was close to or slightly below room temperature. The possibility of  $\text{H}_2\text{O}/\text{D}_2\text{O}$  being lost to the wall of the mixing manifold/reaction cell was investigated by measuring the  $\text{H}_2\text{O}$  concentration using a gas chromatograph fitted with a calibrated pulsed discharge helium ionization detector (PDHID).<sup>29,30</sup>

The concentrations of  $\text{H}_2\text{O}$  after the MFC and after the mixing manifold were, within error, the same, and consequently, it is reasonable to infer that no  $\text{H}_2\text{O}/\text{D}_2\text{O}$  is being lost to the walls of the reaction cell. For each concentration measurement, approximately 20 min was allowed for the flows to reach an equilibrium. When the  $\text{H}_2\text{O}$  isotopes were changed, the apparatus was flushed for at least 24 h. The  $\text{H}_2\text{O}/\text{D}_2\text{O}$  concentrations were varied between 5 and 80 mTorr, ensuring that the pseudo-first-order conditions ( $[\text{CH}] \ll [\text{H}_2\text{O}]$ ) were met.

### III. Results

An example of a typical LIF  $\text{CD}(v=0)$  time profile is shown in Figure 1. The initial exponential growth is consistent with either a “hot” species relaxing to  $\text{CH(D)}(v=0)$  or a hot  $\text{CH(D)}$

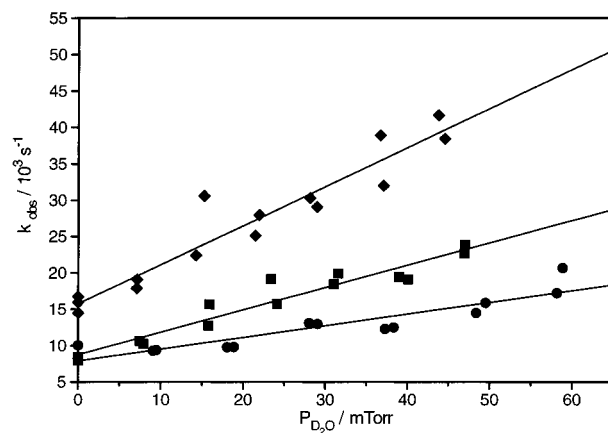


**Figure 2.** Plot of the observed pseudo-first-order rate coefficient,  $k_{\text{obs}}$ , of  $\text{CH}(v=0)$  radicals versus  $\text{D}_2\text{O}$  concentration at various temperatures:  $T = 298$  K ( $\blacklozenge$ );  $T = 383$  K ( $\blacksquare$ );  $T = 473$  K ( $\bullet$ ).

precursor, while the exponential decay is consistent with  $\text{CH(D)}$  reaction with  $\text{H}_2\text{O}/\text{D}_2\text{O}$  and the precursor  $\text{CH(D)Br}_3$ . Experiments were always performed under pseudo-first-order conditions ( $[\text{CH}] \ll [\text{H}_2\text{O}]$ ). The relaxation processes are taken into account by fitting the decay traces to a double exponential equation:

$$[\text{CH}]_t = A \exp(-k_{\text{decay}}t) - B \exp(-k_{\text{growth}}t) \quad (1)$$

where  $k_{\text{decay}}$  corresponds to the pseudo-first-order  $\text{CH}$  reaction rate constant,  $k_{\text{growth}}$  represents the “hot” species relaxation rate constant, and  $k_{\text{growth}} > k_{\text{decay}}$ . Equation 1 is the outcome of a separate study,<sup>23</sup> where we investigated the relaxation in vibrationally excited  $\text{CH(D)}$ . The growth term arises not only from relaxation of higher vibrational states of  $\text{CH}$  but also from another precursor that is formed in the multiphoton photolysis of  $\text{CHBr}_3$ . As a result, the growth term is faster than would be anticipated simply on the basis of vibrational relaxation; in addition, the preexponential term,  $A$ , is larger. To make the analysis tractable, we have adopted the approach summarized in eq 1, in which we describe the post photolysis production of  $\text{CH}(v=0)$  via a single exponential. This is undoubtedly an approximation, since separate exponential terms are needed to describe the formation of  $\text{CH}(v=0)$  from both the first and second vibrational states. Equation 1 essentially rolls these contributions, and that from the additional precursor, into a single exponential. The approximation is quite good, though, since the ratios of the zero time ( $v=0$ ):( $v=1$ ) and ( $v=0$ ):( $v=2$ ) populations are 10 and 20, respectively.<sup>23</sup>

The pseudo-first-order rate coefficient  $k_{\text{decay}}$  increased linearly with  $\text{H}_2\text{O}$  concentration and is given by the following expression:

$$k_{\text{decay}} = k_{\text{bim}}[\text{H}_2\text{O}] + k_{\text{CHBr}_3}[\text{CHBr}_3] \quad (2)$$

where  $k_{\text{bim}}$  is the bimolecular rate coefficient for the reaction with  $\text{H}_2\text{O}$  and  $k_{\text{CHBr}_3}$  is the bimolecular rate coefficient for the reaction with  $\text{CHBr}_3$ . Diffusional loss occurs on a much shorter time scale and can be neglected.

A plot of  $k_{\text{decay}}$  versus  $[\text{H}_2\text{O}]$  yields a straight line with the gradient equal to  $k_{\text{bim}}$ . An example of typical bimolecular plots for the reaction of  $\text{CH}$  with  $\text{D}_2\text{O}$  at various temperatures is shown in Figure 2. The experiments were performed on all four isotopic variants of the  $\text{CH} + \text{H}_2\text{O}$  reaction in the temperature range between 291 and 723 K. Normally, 14–15 experiments were performed with varying water concentrations at each

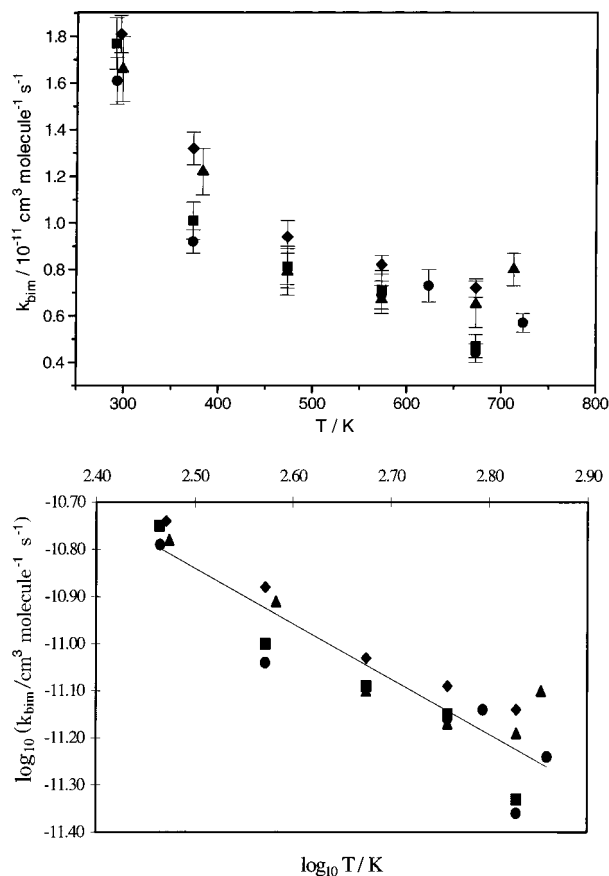


**Figure 3.** Temperature dependence of the bimolecular rate coefficient,  $k_{\text{bim}}$ , for the reactions CH + H<sub>2</sub>O (■), CH + D<sub>2</sub>O (▲), CD + H<sub>2</sub>O (●), and CD + D<sub>2</sub>O (◆). (a) Plot of the  $k_{\text{bim}}$  versus temperature and (b) plot of  $\log k_{\text{bim}}$  versus  $\log$  temperature.

reaction and temperature. The results for the bimolecular rate coefficients as a function of temperature are shown in Figure 3 and are also listed in Table 1. The quoted errors correspond to  $\pm 1\sigma$  with the standard deviation given by a linear least-squares fit to the bimolecular plot. The systematic error will be higher due to uncertainties in the concentration determination of H<sub>2</sub>O and is estimated to be approximately  $\pm 20\%$ . When the temperature dependence was fitted, the data were weighted by  $1/\sigma^2$  using the 20% error as  $\sigma$ . The observed rate coefficient was independent of pressure in the range 20–200 Torr helium within the experimental error (see Table 1).

The reactions of CH and CD with H<sub>2</sub>O and D<sub>2</sub>O exhibit a negative temperature dependence with the rate coefficient decreasing by approximately 65% over the investigated temperature range. All isotopic variants appear, within experimental error, to react with the same rate. Deuteration of either the CH radical or the H<sub>2</sub>O has no effect on the kinetics. The data can be fitted to  $AT^n$  with  $n \approx -1.2$ . An Arrhenius fit yields a negative activation energy of  $E_a \approx -4 \text{ kJ mol}^{-1}$ . The parameters for both fits can be found in Table 2.

In addition to the experiments on CH radicals in their vibrational ground state, the removal of CH( $\nu=1$ ) and CD( $\nu=1,2$ ) with H<sub>2</sub>O and D<sub>2</sub>O at room temperature was also investigated. The results obtained are shown in Table 3. All isotopic variants show an increase in the rate coefficient for the higher vibrational states of CH and CD. While the enhancement in the rate coefficient on going from  $\nu = 0$  to  $\nu = 1$  is only ca. 25–40% for the CH(D) + H<sub>2</sub>O reaction, it is much more significant for the reaction of CH(D) + D<sub>2</sub>O (75–90%).

**TABLE 1: Experimental Results<sup>a</sup>**

(a) CH + H <sub>2</sub> O → Products		
<i>T</i> /K	[H <sub>2</sub> O]/10 <sup>14</sup> molecule cm <sup>-3</sup>	<i>k</i> /10 <sup>-11</sup> cm <sup>3</sup> molecule <sup>-1</sup> s <sup>-1</sup>
291 (70 Torr)	2.2–13.6	1.77 ± 0.11
293 (200 Torr)	7.1–45.6	1.27 ± 0.19
373	1.8–11.5	1.01 ± 0.08
473	1.4–8.9	0.81 ± 0.08
573	1.8–11.6	0.71 ± 0.08
673	1.8–11.2	0.47 ± 0.05
(b) CH + D <sub>2</sub> O → Products		
<i>T</i> /K	[D <sub>2</sub> O]/10 <sup>14</sup> molecule cm <sup>-3</sup>	<i>k</i> /10 <sup>-11</sup> cm <sup>3</sup> molecule <sup>-1</sup> s <sup>-1</sup>
298	2.3–14.4	1.66 ± 0.14
383	1.9–11.8	1.22 ± 0.10
473	1.8–12.0	0.79 ± 0.10
573	2.0–12.9	0.67 ± 0.06
673	1.7–11.3	0.65 ± 0.10
713	1.8–11.1	0.80 ± 0.07
(c) CD + H <sub>2</sub> O → Products		
<i>T</i> /K	[H <sub>2</sub> O]/10 <sup>14</sup> molecule cm <sup>-3</sup>	<i>k</i> /10 <sup>-11</sup> cm <sup>3</sup> molecule <sup>-1</sup> s <sup>-1</sup>
291 (20 Torr)	2.7–17.2	1.44 ± 0.05
292 (70 Torr)	2.5–16.8	1.27 ± 0.07
292 (130 Torr)	3.6–24.2	1.61 ± 0.10
373	1.9–12.8	0.92 ± 0.05
473	2.6–17.0	0.81 ± 0.09
573	2.6–17.6	0.69 ± 0.06
623	2.2–14.3	0.73 ± 0.07
673	2.3–14.1	0.44 ± 0.04
723	1.9–12.3	0.57 ± 0.04
(d) CD + D <sub>2</sub> O → Products		
<i>T</i> /K	[D <sub>2</sub> O]/10 <sup>14</sup> molecule cm <sup>-3</sup>	<i>k</i> /10 <sup>-11</sup> cm <sup>3</sup> molecule <sup>-1</sup> s <sup>-1</sup>
296	1.9–12.5	1.81 ± 0.08
373	1.5–9.5	1.32 ± 0.07
473	1.8–11.5	0.94 ± 0.07
573	2.1–13.7	0.82 ± 0.04
673	1.8–11.5	0.72 ± 0.04

<sup>a</sup> Errors correspond to  $\pm 1\sigma$  SD.

**TABLE 2: Temperature Dependence of the Reactions CH/CD + H<sub>2</sub>O/D<sub>2</sub>O<sup>a</sup>**

system	$k(T) = A(T/298)^n$		$k(T) = B \exp(-E_A/RT)$	
	<i>A</i> /10 <sup>-11</sup> cm <sup>3</sup> s <sup>-1</sup>	<i>n</i>	<i>B</i> /10 <sup>-12</sup> cm <sup>3</sup> s <sup>-1</sup>	<i>E<sub>A</sub></i> /kJ mol <sup>-1</sup>
CH + H <sub>2</sub> O	1.56 ± 0.25	-1.42 ± 0.31	2.14 ± 0.62	-5.07 ± 1.19
CH + D <sub>2</sub> O	1.49 ± 0.25	-1.04 ± 0.29	3.40 ± 0.87	-3.85 ± 1.10
CD + H <sub>2</sub> O	1.38 ± 0.21	-1.16 ± 0.25	2.67 ± 0.62	-4.23 ± 1.01
CD + D <sub>2</sub> O	1.71 ± 0.28	-1.13 ± 0.32	3.43 ± 1.01	-4.10 ± 1.22

<sup>a</sup> Errors correspond to  $\pm 1\sigma$  SD given by a non-linear least-squares fit. The data were weighted by  $1/\sigma^2$  using a  $\sigma$  of 20%.

**TABLE 3: Dependence of the Rate Coefficient on the Vibrational State at *T* = 293 K<sup>a</sup>**

	CH + H <sub>2</sub> O <i>k</i> /10 <sup>-11</sup> cm <sup>3</sup> s <sup>-1</sup>	CH + D <sub>2</sub> O <i>k</i> /10 <sup>-11</sup> cm <sup>3</sup> s <sup>-1</sup>	CD + H <sub>2</sub> O <i>k</i> /10 <sup>-11</sup> cm <sup>3</sup> s <sup>-1</sup>	CD + D <sub>2</sub> O <i>k</i> /10 <sup>-11</sup> cm <sup>3</sup> s <sup>-1</sup>
$\nu = 0$	1.77 ± 0.11	1.66 ± 0.14	1.61 ± 0.10	1.81 ± 0.08
$\nu = 1$	2.19 ± 0.14	3.21 ± 0.22	2.22 ± 0.08	3.15 ± 0.27
$\nu = 2$			3.29 ± 0.20	3.32 ± 0.23

<sup>a</sup> Errors correspond to  $\pm 1\sigma$  SD.

#### IV. Discussion

The reaction CH + H<sub>2</sub>O has been investigated previously as a function of temperature by Zabarnick et al.<sup>20</sup> using a similar

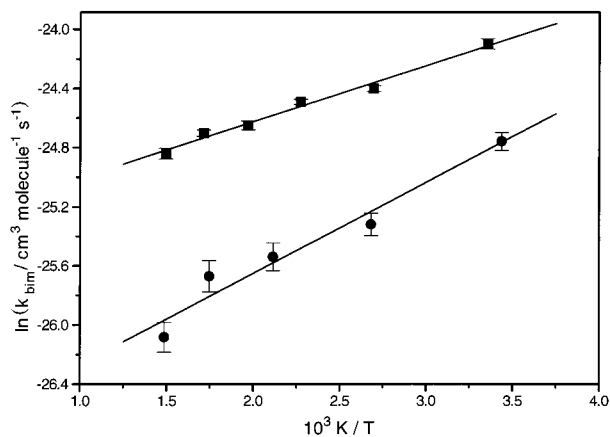


**Figure 4.** Arrhenius plot for the reaction  $\text{CH} + \text{H}_2\text{O}$ : this work (●); ref 20 (■).

experimental technique. They diluted  $\text{H}_2\text{O}$  with argon in large storage bulbs and calculated its concentration from the partial pressure. Their results are compared with our values in Figure 4, which represents the two sets of data in an Arrhenius form. Our absolute rate coefficients are typically about a factor of 2 lower. Experimental determinations of water vapor concentrations in kinetic studies are notoriously difficult due to loss of water to the surface of storage vessels or delivery tubing. A variety of methods have been used to overcome this problem. Our approach has been to generate a saturated vapor, thus avoiding storage loss, to monitor saturation using a humidity probe and to check relative concentrations along the delivery system by gas chromatography. One interpretation of the discrepancy between our results and those of Zabarnick et al.<sup>20</sup> is that water losses occurred in our system. The extensive checks that we conducted, as outlined above, argue that this was not the case. The negative temperature dependence for the  $\text{CH} + \text{H}_2\text{O}$  reaction is slightly steeper, but the other three isotopic variations of this reaction seem to follow the same trend as found by Zabarnick et al.,<sup>20</sup> so that there is a satisfying agreement in the activation energy. Bosnali and Perner<sup>21</sup> studied the  $\text{CH} + \text{H}_2\text{O}$  reaction at room temperature. Their value is about a factor of 2.5 higher than our room-temperature rate coefficient. It should be noted that the Bosnali and Perner<sup>21</sup> data on  $\text{CH} + \text{CH}_4$ , which are from the same reference as their  $\text{CH} + \text{H}_2\text{O}$  data, also disagree with recent measurements on the  $\text{CH} + \text{CH}_4$  reaction.<sup>14,16</sup>

The observed negative temperature dependence has also been found in reactions of  $\text{CH}$  with hydrocarbons.<sup>19</sup> Such a temperature dependence is found in many barrierless reactions and its dependence on aspects of the potential energy surface has been examined by Pesa et al.<sup>31</sup> using canonical flexible transition state theory (CFTST). The interplay between the decrease in potential energy as the radicals approach, and the change in character of the *transitional* modes of motion from free to hindered rotations generates a minimum in the partition function for the collision complex, and the transition state is located at this minimum. As the temperature and the average energy of the complex increase, the transition state moves to smaller distances where the rotors are more hindered and the partition function falls still further, generating a negative temperature dependence in the rate constant.

It has been shown that  $\text{CH}$  radicals undergo rapid insertion reactions with alkanes.<sup>19</sup> The thermodynamic values of the feasible pathways for the  $\text{CH} + \text{H}_2\text{O}$  reaction are shown in Figure 5 and are also listed in Table 4. It shows that insertion is the most exothermic of the pathways and results in a “hot”

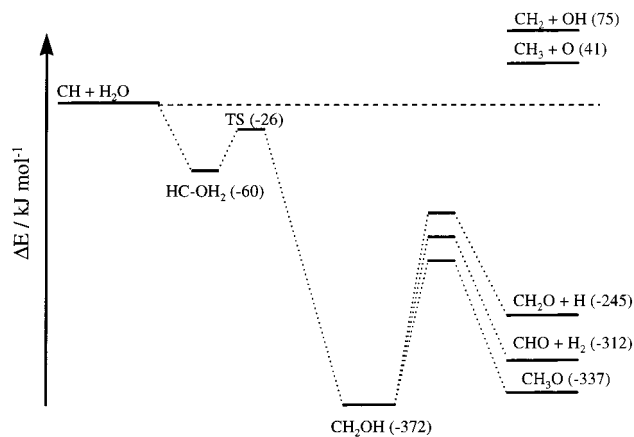


**Figure 5.** Schematic diagram of the potential energy surface for the reaction  $\text{CH} + \text{H}_2\text{O}$ . The energies of the intermediate complex and the insertion transition state (TS) are taken from Wang et al.<sup>22</sup>

**TABLE 4: Heats of Formation of Some Species Involved in the  $\text{CH} + \text{H}_2\text{O}$  Reaction Mechanism<sup>a</sup>**

	CH	H <sub>2</sub> O	CH <sub>2</sub>	OH	CH <sub>3</sub>	O
$\Delta_f H^\circ_{298}$	596.4	-241.1	390.4	39.3	146.4	249.2
ref	32	33	32	33	32	34
	CH <sub>2</sub> O	H	CHO	H <sub>2</sub>	CH <sub>3</sub> O	CH <sub>2</sub> OH
$\Delta_f H^\circ_{298}$	-108.6	218.0	43.1	0	17.2	-17.8
ref	33	34	35		32	36

<sup>a</sup>  $\Delta_f H^\circ_{298}$  is given in units of  $\text{kJ mol}^{-1}$ .

hydroxymethyl radical, which possesses  $372 \text{ kJ mol}^{-1}$  excess energy, and therefore may decompose to  $\text{CH}_2\text{O} + \text{H}$  ( $\Delta_R H^\circ = -245 \text{ kJ mol}^{-1}$ ) or isomerize to a methoxy radical ( $\Delta_R H^\circ = -337 \text{ kJ mol}^{-1}$ ), as well as being stabilized by the buffer gas. Formation of  $\text{HCO} + \text{H}_2$  is also energetically feasible. The high exothermicity of the fragmentation channels suggests that stabilization of  $\text{CH}_2\text{OH}$  or of  $\text{CH}_3\text{O}$  is unlikely. Detailed calculations for the  $\text{CH} + \text{CH}_4$  reaction, using master equation techniques,<sup>14</sup> showed that stabilization of the ethyl intermediate complex is only significant under extreme conditions (i.e., above  $10^5$  Torr). The  $\text{CH} + \text{CH}_4$  reaction shows an isotope effect where deuteration of the methane results in a reduction of the rate coefficient by ca. 30% over the entire temperature range. No isotope effect was observed in the present experiments. All isotopic variants of the  $\text{CH} + \text{H}_2\text{O}$  reaction appear to react with the same rate coefficient, suggesting a somewhat different mechanism from the direct insertion reaction postulated for  $\text{CH} + \text{CH}_4$ .

Figure 5 shows a schematic diagram of the potential energy for the  $\text{CH} + \text{H}_2\text{O}$  reaction that can be used to rationalize our experimental data. Wang et al.<sup>22</sup> performed ab initio molecular orbital calculations incorporating electron correlation with Møller–Plesset perturbation theory at the UMP2/3-21G and UMP2/6-31G\*\* levels on this system. They confirmed the insertion mechanism, but additionally they found, in the calculated reaction path, an intermediate complex prior to the transition state that is  $60 \text{ kJ mol}^{-1}$  lower in energy than the reactants. The molecular orbital interaction analysis implies that this intermediate complex is due to the donation of one lone electron pair on the O-atom to the empty carbon *p*-orbital of the  $\text{CH}$  radical. This intermediate complex then subsequently rearranges to form the insertion adduct between  $\text{CH} + \text{H}_2\text{O}$ , the hydroxymethyl radical, which itself can proceed to the reaction products, as discussed above. The isotope data imply that it is the formation of the intermediate complex that is rate determining.

The channels to form CH<sub>2</sub> + OH and CH<sub>3</sub> + O are endothermic by 75 and 41 kJ mol<sup>-1</sup>, respectively. As these channels must have activation energies at least equal to their endothermicities, the observed negative temperature dependence suggests that these channels are not operating. The increase in the rate coefficient for the higher vibrational states ( $\nu = 1, 2$ ) might indicate that these abstraction channels are opening up, although the additional energy in the vibrationally excited states is still not sufficient fully to overcome the endothermicity of the reaction. In addition, experiments were performed where the production of OH radicals was monitored. A constant signal from OH was observed, but its source was photolytic. No OH could be assigned to a CH reaction. It appears that the possibility of the endothermic channels opening up can be ruled out under the conditions studied.

An explanation still needs to be found for the enhanced rate coefficients of CH and CD in their  $\nu = 1$  and  $\nu = 2$  vibrational states. Vibrational enhancement in pressure dependent reactions between species capable of forming a strong chemical bond has been associated in previous work with the attainment of the high-pressure limit,<sup>37</sup> e.g., in the reactions of CH with H<sub>2</sub><sup>9</sup> and CH with N<sub>2</sub>.<sup>11</sup> The absence of a pressure dependence in the reaction of CH with H<sub>2</sub>O seems to argue against this explanation in the present context. However, the complex is quite weakly bound (60 kJ mol<sup>-1</sup>) and the lifetime with respect to dissociation may be sufficiently short that pressures substantially higher than those used here are necessary for stabilization to compete. While the barrier to dissociation to generate products is lower than that for the reverse dissociation to regenerate the reactants, the transition state is tight and it is entirely feasible that reverse dissociation is competitive. For vibrationally excited CH, reverse dissociation would form CH( $\nu=0$ ), so that the true high-pressure association rate coefficient would be obtained, as with CH + H<sub>2</sub> and N<sub>2</sub>. Enhancement of the rate coefficient for a vibrationally excited reagent has been found for the reaction of CH with CO<sub>2</sub>,<sup>10</sup> which is also not pressure dependent, and a similar explanation may apply.

An alternative mechanism is a physical relaxation process. The magnitude of the rate coefficients suggests resonant V–V transfer. The CH( $\nu=1$ ) and CD( $\nu=1$ ) vibrational wavenumbers are 2732<sup>24</sup> and 2032 cm<sup>-1</sup>,<sup>25</sup> respectively, and those for H<sub>2</sub>O and D<sub>2</sub>O are 1595, 3657, 3756 cm<sup>-1</sup> and 1178, 2666, 2789 cm<sup>-1</sup>, respectively.<sup>38</sup> This relaxation process does appear to have some correlation with how close the systems are to resonance; the CH + D<sub>2</sub>O system has the best resonance at around 2700 cm<sup>-1</sup> and has the largest rate coefficient of the four studied reactions in the  $\nu = 1$  state. However, it is clear that resonant V–V transfer cannot provide a *general* explanation of the high rate coefficients of the vibrationally excited states<sup>39</sup>, although it may be significant in CH + D<sub>2</sub>O.<sup>40</sup> In a related study, we have noted comparatively facile vibrational relaxation of CH by nonpolar gases.<sup>23</sup> It may be that the observed high rate coefficients are related to the interaction between the lone pair on the oxygen of H<sub>2</sub>O and the *p*-orbital of the CH, as discussed by Wang et al.,<sup>22</sup> which facilitates V–V transfer.

It is also interesting to compare the absolute magnitudes of the rate coefficients of CH with various hydrides. Our rate coefficient data for CH with H<sub>2</sub>O are consistent with the theoretical description that the reaction initially proceeds via a complex; the interpretation of no kinetic isotope is that complex formation is rate determining. The reactions of CH with NH<sub>3</sub> and CH<sub>3</sub>OH also have the possibility of proceeding via a complex. The complex between CH and NH<sub>3</sub> has been identified in the calculations of Wang et al.<sup>22</sup> Therefore, if complex

**TABLE 5: Correlation of the Ionization Potential (IP) of Various Hydrides and Their Rate Coefficients with CH Radicals<sup>a</sup>**

	NH <sub>3</sub>	CH <sub>3</sub> OH	CH <sub>4</sub>	H <sub>2</sub> O
IP/eV	10.16	10.85	12.51	12.61
<i>k</i> /cm <sup>3</sup> s <sup>-1</sup>	2.0 × 10 <sup>-10</sup>	2.2 × 10 <sup>-10</sup>	9.8 × 10 <sup>-11</sup> <sup>a</sup>	1.8 × 10 <sup>-11</sup>

<sup>a</sup> The rate coefficient for the reaction CH + CH<sub>4</sub> needs to be divided by 4 in order to correct for the reaction path degeneracy.

formation is rate determining for these three reactions, then the magnitude of the rate coefficient should be related to the availability of the lone electron pair on the hydride, which is involved in the bonding of the complex.<sup>22</sup> A measure of the availability of the lone pair is the ionization potential, and as shown in Table 5, there is a good correlation between the measured rate coefficient and the ionization potential (IP). NH<sub>3</sub> has an IP of 10.16 eV<sup>41</sup> and a rate coefficient with CH of 2.0 × 10<sup>-10</sup> cm<sup>3</sup> molecule<sup>-1</sup> s<sup>-1</sup>,<sup>40</sup> close to the limiting gas kinetic collision frequency. CH<sub>3</sub>OH has an IP of 10.85 eV,<sup>41</sup> similar to NH<sub>3</sub>, and the rate coefficient with CH, which has been determined just recently in our group, is also close to the gas kinetic collision frequency ( $k = 2.2 \times 10^{-10}$  cm<sup>3</sup> molecule<sup>-1</sup> s<sup>-1</sup>).<sup>42</sup> The same study revealed no kinetic isotope effect for the reaction of CH<sub>3</sub>OH with CH, consistent with complex formation. H<sub>2</sub>O has an IP of 12.61 eV,<sup>41</sup> which is significantly higher than the IPs of the other hydrides, and a rate coefficient with CH about an order of magnitude slower ( $k = 1.8 \times 10^{-11}$  cm<sup>3</sup> molecule<sup>-1</sup> s<sup>-1</sup>).

This correlation between the rate coefficient and the IP of the hydride appears to add support to the idea that these reactions proceed via a complex formation (see Table 5). It is interesting to note that the reaction with CH<sub>4</sub> also fits in with the correlation. CH<sub>4</sub> has an IP of 12.51 eV,<sup>41</sup> similar to H<sub>2</sub>O. The reaction path degeneracy must be accommodated in this comparison, since CH can interact with four C–H  $\sigma$  bonds, giving a rate coefficient per bond of  $2.5 \times 10^{-11}$  cm<sup>3</sup> molecule<sup>-1</sup> s<sup>-1</sup>.<sup>14</sup> However, CH<sub>4</sub> does not possess a lone-pair electron and consequently cannot form an intermediate complex.

While the results from this study allow us to better extrapolate the rate coefficient of the CH + H<sub>2</sub>O reaction to higher, combustion relevant, temperatures, it is the lack of knowledge on the products of this reaction that limits accurate modeling under combustion conditions. A product investigation, either via experiment or calculation, is needed to fully elucidate the mechanism of the CH + H<sub>2</sub>O reaction.

## V. Conclusions

The rate coefficients for the reactions of CH( $\nu=0$ ) and CD( $\nu=0$ ) radicals with the combustion species H<sub>2</sub>O and D<sub>2</sub>O have been measured in the temperature range between 291 and 723 K for all four isotopic variants. The reactions exhibit a negative temperature dependence and appear to show no isotope effect. These observations taken together suggest that the reaction does not proceed via direct insertion in the O–H(D) bond, but via the formation of an intermediate complex between CH and H<sub>2</sub>O, followed by rearrangement to the overall insertion product, CH<sub>2</sub>OH. The reaction is independent of total pressure between 20 and 200 Torr at room temperature. Vibrational excitation (CH( $\nu=1$ ) and CD( $\nu=1,2$ )) resulted in an enhancement of the rate coefficient.

**Acknowledgment.** We are grateful to a referee for valuable comments on the mechanism of vibrational rate enhancement. Financial support of the EC HCM program, EPSRC, and Zonta International (M.P.) is acknowledged.

## References and Notes

- (1) Fenimore, C. P. *Thirteenth Symposium (International) on Combustion*; The Combustion Institute, Pittsburgh, PA, 1971; p 373.
- (2) Miller, J. A.; Bowman, C. T. *Prog. Energy Combust. Sci.* **1989**, *15*, 287.
- (3) Miller, J. A.; Kee, R. J.; Westbrook, C. *Annu. Rev. Phys. Chem.* **1990**, *41*, 345.
- (4) Wayne, R. P. *Chemistry of Atmospheres*, 2nd ed.; Clarendon Press: Oxford, U.K., 1991.
- (5) Gladstone, G. R.; Allen, M.; Yung, Y. L. *Icarus* **1996**, *119*, 1.
- (6) Romani, P. N.; Bishop, J.; Bezaud, B.; Atreya, S. *Icarus* **1993**, *106*, 442.
- (7) Sanders, W. A.; Lin, M. C. In *Chemical Kinetics and Small Organic Radicals*; Alfassi, Z., Ed.; CRC Press: Boca Raton, FL, 1988; Vol. 3, p 108.
- (8) (a) Fulle, D.; Hippler, H. *J. Chem. Phys.* **1996**, *105*, 5423. (b) Fulle, D.; Hippler, H. *J. Chem. Phys.* **1997**, *106*, 8691.
- (9) Brownsword, R. A.; Canosa, A.; Rowe, B. R.; Sims, I. R.; Smith, I. W. M.; Stewart, D. W. A.; Symonds, A. C.; Travers, D. *J. Chem. Phys.* **1997**, *106*, 7662.
- (10) Mehlmann, C.; Frost, M. J.; Heard, D. E.; Orr, B. J.; Nelson, P. F. *J. Chem. Soc., Faraday Trans.* **1996**, *92*, 2335.
- (11) Herbert, L. B.; Canosa, A.; Rowe, B. R.; Sims, I. R.; Smith, I. W. M.; Stewart, D. W. A.; Symonds, A. C. *J. Phys. Chem.* **1996**, *100*, 14928.
- (12) Brownsword, R. A.; Herbert, L. B.; Smith, I. W. M.; Stewart, D. W. A. *J. Chem. Soc., Faraday Trans.* **1996**, *92*, 2335.
- (13) (a) Taatjes, C. A. *J. Phys. Chem.* **1996**, *100*, 17840. (b) Taatjes, C. A. *J. Chem. Phys.* **1997**, *106*, 1786.
- (14) Blitz, M. A.; Johnson, D. G.; Pesa, M.; Pilling, M. J.; Robertson, S. H.; Seakins, P. W. *J. Chem. Soc., Faraday Trans.* **1997**, *93*, 1473.
- (15) Berman, M. R.; Lin, M. C. *Chem. Phys.* **1983**, *82*, 435.
- (16) Thiesemann, H.; MacNamara, J.; Taatjes, C. A. *J. Phys. Chem. A* **1997**, *101*, 1881.
- (17) Canosa, A.; Sims, I. R.; Travers, D.; Smith, I. W. M.; Rowe, R. B. *Astronomy Astrophys.* **1997**, *323*, 644.
- (18) Wang, Z. X.; Huang, M. B.; Liu, R. Z. *Can. J. Chem.* **1997**, *75*, 996.
- (19) (a) Zabarnick, S.; Fleming, J. W.; Lin, M. C. *Chem. Phys.* **1987**, *112*, 409. (b) Zabarnick, S.; Fleming, J. W.; Lin, M. C. *J. Chem. Phys.* **1988**, *88*, 5983.
- (20) Zabarnick, S.; Fleming, J. W.; Lin, M. C. *21st Symposium (International) on Combustion*; The Combustion Institute: Pittsburgh, PA, 1986; p 713.
- (21) Bosnali, M. W.; Perner, D. Z. *Naturforsch.* **1971**, *26A*, 1768.
- (22) Wang, Z.-X.; Liu, R.-Z.; Huang, M.-B.; Yu, Z.-H. *Can. J. Chem.* **1996**, *74*, 910.
- (23) Blitz, M. A.; Pesa, M.; Pilling, M. J.; Seakins, P. W. To be submitted.
- (24) Gerö, L. Z. *Phys.* **1941**, *118*, 27.
- (25) Gerö, L. Z. *Phys.* **1941**, *117*, 709.
- (26) Herzberg, G.; Johns, J. W. C. *Astrophys. J.* **1969**, *158*, 399.
- (27) Lide, D. R., Ed. *CRC Handbook of Chemistry and Physics*; CRC Press: Boca Raton, FL, 1988–1989.
- (28) Combs, R. L.; Googin, J. M.; Smith, H. A. *J. Phys. Chem.* **1954**, *58*, 1000.
- (29) (a) Wentworth, W. E.; Vasin, S. V.; Stearns, S. D.; Meyer, C. J. *Chromatographia* **1992**, *34*, Nos. 5–8, 219. (b) Wentworth, W. E.; Qin, Y.; Wiedeman, S.; Stearns, S. D.; Madabushi, J. *Appl. Spectrosc.* **1995**, *49*, No. 9, 1282.
- (30) Hunter, M. C.; Bartle, K. D.; Lewis, A. C.; McQuaid, J. B.; Myers, P.; Seakins, P. W.; Van Tilburg, C. *J. High Res. Chromatogr.* **1998**, *21*, 75.
- (31) Pesa, M.; Pilling, M. J.; Robertson, S. H.; Wardlaw, D. *J. Phys. Chem.* **1998**, *102*, 8526.
- (32) Kerr, J. A. *Strengths of Chemical Bonds in Handbook of Chemistry and Physics*, 77th ed.; Lide, D. R., Ed.; CRC Press: Boca Raton, FL, 1996–1997.
- (33) Burcat, A.; McBride, B. *1997 Ideal Gas Thermodynamic Data for Combustion and Air-Pollution Use*; Technion Aerospace Engineering (TAE) Report No. 804; Technion Aerospace Engineering, Israel Institute of Technology: Haifa, Israel, 1997.
- (34) Kee, R. J.; Rupley, F. M.; Miller, F. A. *The Chemkin Thermodynamic Data Base*; Sandia Report No. Sand87-8215B; UC-4, Sandia National Laboratories: New Mexico, 1990.
- (35) Chuang, M. C.; Folz, M. F.; Moore, C. B. *J. Chem. Phys.* **1987**, *87*, 3855.
- (36) Johnson, R. D.; Hudgens, J. W. *J. Phys. Chem.* **1996**, *100*, 19874.
- (37) Smith, I. W. M. *J. Chem. Soc., Faraday Trans.* **1997**, *93*, 3741.
- (38) Herzberg, G. *Electronic Spectra and Electronic Structure of Polyatomic Molecules*; Van Nostrand Reinhold Co.: New York, 1966.
- (39) Lambert, J. D. *Vibrational and Rotational Relaxation in Gases*; Clarendon Press: Oxford, U.K., 1977.
- (40) Becker, K. H.; Engelhardt, B.; Geiger, H.; Kurtenbach, R.; Wiesen, P. *Chem. Phys. Lett.* **1993**, *210*, 135.
- (41) Lide, D. R., Ed. *CRC Handbook of Chemistry and Physics*, 75th ed.; CRC Press: Boca Raton, FL, 1994–1995.
- (42) Seakins, P. W.; Johnson, D. G. Private communication.